

Evolution of Electronic Structure Across the Rare-Earth RNiO₃ Series

John W. Freeland

Advanced Photon Source, Argonne National Laboratory, Argonne, Illinois 60439, USA

Michel van Veenendaal

*Department of Physics, Northern Illinois University, DeKalb, Illinois 60115, USA and
Advanced Photon Source, Argonne National Laboratory, Argonne, Illinois 60439, USA*

Jak Chakhalian

Department of Physics, University of Arkansas, Fayetteville, Arkansas 70701, USA

(Dated: March 2, 2024)

The perovskite rare-earth nickelates, RNiO₃ (R=La ... Lu), are a class of materials displaying a rich phase-diagram of metallic and insulating phases associated with charge and magnetic order. Being in the charge transfer regime, Ni³⁺ in octahedral coordination displays a strong hybridization with oxygen to form $3d - 2p$ mixed states, which results in a strong admixture of $3d^8 \underline{L}$ into $3d^7$, where \underline{L} denotes a hole on the oxygen. To understand the nature of this strongly hybridized ground state, we present a detailed study of the Ni and O electronic structure using high-resolution soft X-ray Absorption Spectroscopy (XAS). Through a comparison of the evolution of the XAS line-shape at Ni L- and O K-edges across the phase diagram, we explore the changes in the electronic signatures in connection with the insulating and metallic phases that support the idea of hybridization playing a fundamental role.

I. INTRODUCTION

Complex oxides offer a diverse range of phenomena that span magnetism to superconductivity to colossal response at phase transitions[1, 2]. Of particular interest here is understanding why materials undergo a conversion from metallic to insulating phases[3]. Nickelates form an intriguing case for materials that undergo a metal-to-insulator transition (MIT) connected to the onset of charge and magnetic order. As is encountered in other complex oxides with multiple degrees of freedom, the underlying cause can be difficult to unravel[4, 5].

The case of RNiO₃ has been well studied for several decades as a case of charge and magnetic order associated with a metal to insulator transition (MIT) for the late 3d transition metal oxides[7–11]. Originally, it was expected that the Jahn-Teller active Ni³⁺ ($3d^7$) state should demonstrate orbital order[12, 13], but this was ruled out in the favor of a charged ordered (CO) phase both experimentally[14, 15] and theoretically[16–19]. The magnetic state was characterized early on as E'-type antiferromagnetic (AFM) order with a $4 \times 4 \times 4$ monoclinic unit cell with large and small moment Ni sites arrange in an -up-up-down-down- pattern[12, 20]; a definitive assigning the moment orientations has proven to be difficult with powder samples. Later, scattering experiments on relaxed NdNiO₃ thin films measured at the Ni L₃ resonance supported a spiral structure[21, 22] and when extended to powder samples showed the same resonant response in the soft X-rays possibly indicating the same magnetic structure[23, 24]. While scattering probes showed a clear ordering of the local magnetic moments, magnetic properties explored by other methods illustrated a complex crossover of the magnetic state from Pauli like to Curie-Weiss type[25]. Recent total moment methods found the evidence for spin-canting[26]. Additionally, experiments on LaNiO₃ emphasized the difficulty in understanding the total magnetic

moment due to strong electron-electron correlations[27].

On the electronic side, the trends across the series were connected with the decreasing band-width as one moves to smaller R ions[6, 11, 28, 29], which was also early on associated with a change in the $p - d$ covalency[30] that has a consequence of moving the boundary between metal and insulator in the Zaanen-Sawatzky-Allen (ZSA) diagram for charge-transfer compounds[31]. Photoemission[32–35] and optical[36] measurements also showed that the gap is quite small (100 - 200 meV). Early on it was recognized that the charge-transfer nature of the compounds played an important role in the physics[4, 37], which indicated that Ni³⁺ contained more of $3d^8 \underline{L}$ character than $3d^7$, where \underline{L} denotes a ligand hole on the oxygen site. This was explored in more detail by Mizokawa et al.[16] and further supported by recent advances in theoretical approaches for strongly correlated electron states[17–19, 38, 39]. These findings support the view that the charge order is more likely *oxygen-site* or bond centered ($3d^8 \underline{L} + 3d^8 \underline{L} \rightarrow 3d^8 + 3d^8 \underline{L}^2$) rather than the Ni site centered picture ($3d^7 + 3d^7 \rightarrow 3d^{7-\delta} + 3d^{7+\delta}$).

In this article, we explore the detailed evolution of the nickel and oxygen electronic structure throughout the phase diagram above and below the MIT and AFM ordering transitions by using spectroscopic probes at the Ni L-edge and Oxygen K-edge to track the evolution of the electronic structures to understand the underlying physics.

II. EXPERIMENTAL DETAILS

Bulk RNiO₃ samples were studied in the powder form and the details of high-pressure oxygen synthesis are discussed elsewhere[29]. X-ray absorption measurements were undertaken at beamline 4-ID-C of the Advanced Photon Source and were simultaneously recorded by surface sensitive total electron yield (EY) and bulk-sensitive partial fluorescence yield

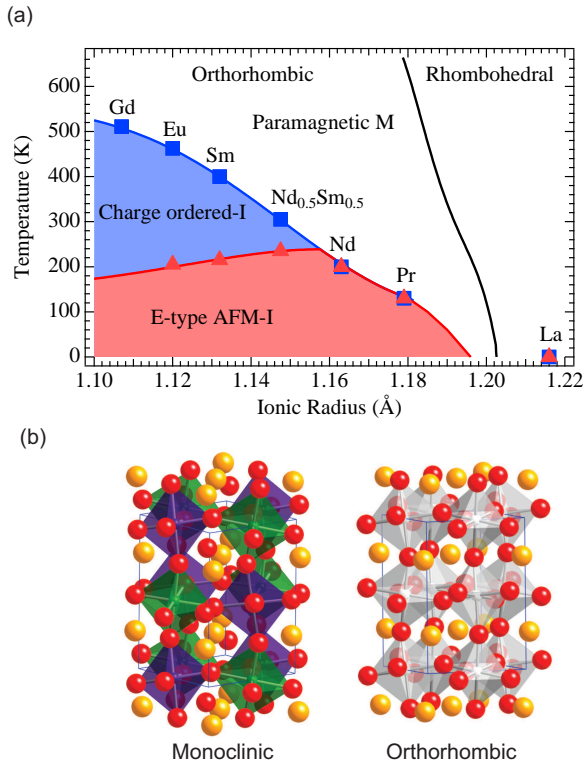


FIG. 1: (a) Bulk RNiO_3 phase diagram for the series of samples explored in this paper. Data is from Ref. [6] (b) Crystal structures for the low-temperature charge-ordered monoclinic and high-temperature metallic orthorhombic phases.

(FY) modes. In addition, a NiO sample was positioned upstream of the experiment and recorded during every scan to perform alignment between samples with up to 50 meV precision. Powder samples were mounted on electrically conducting carbon tape. Excellent agreement between EY and FY measurements indicates no degradation of the surface with respect to the bulk phase. The beamline resolution was 100 meV at the oxygen K-edge and 200 meV at the Ni-L edge.

III. RESULTS

A. Ni L-edge Absorption

In this section we present a summary of the Ni L-edge X-ray absorption, which is an excitation from the Ni $2p$ core state to the unoccupied Ni $3d$ states just above the Fermi level. Figure 2 shows the L_3 portion of the spectra in both EY (a) and FY (b). Aside from the strong self-absorption of the FY spectra, there is a very good correspondence of the spectral features across the series from $R = \text{Gd}$ to La. Aside from the overlap with the strong La M_4 line for LaNiO_3 , the spectra show a clear evolution across the series as one moves across the metal-insulator transition. These spectra are in good agreement with previous measurements on bulk RNiO_3 [37, 40]. The spectra are qualitatively described by a sharp multiplet

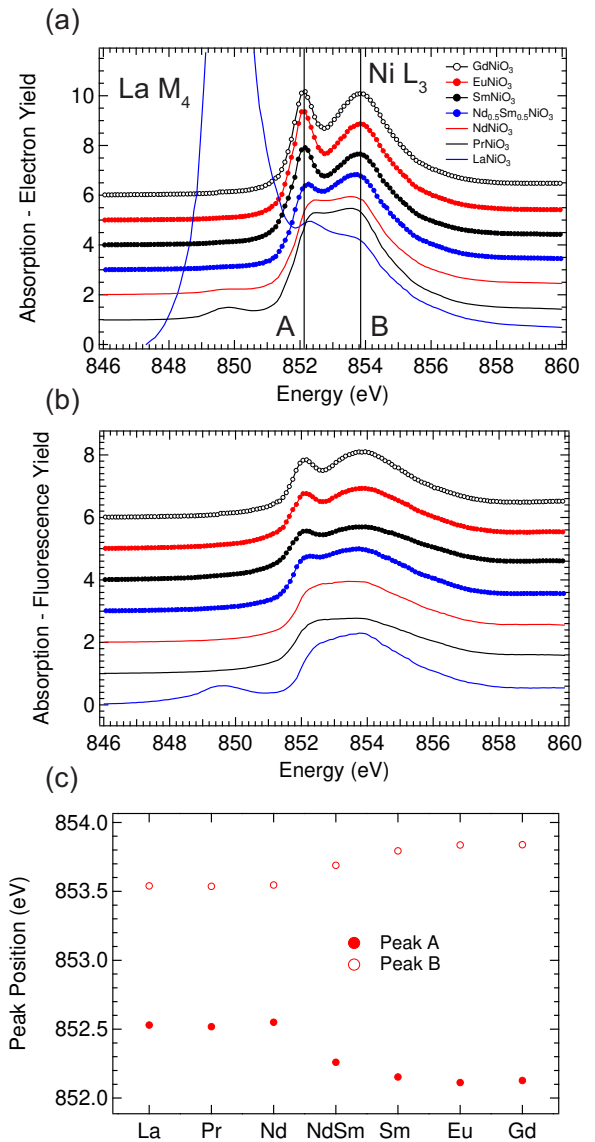


FIG. 2: Ni L_3 absorption data at 300 K acquired in (a) surface sensitive EY and (b) bulk sensitive FY across the series from $R = \text{Gd}$ to La. Panel (c) shows the multiplet peak splitting that is discussed in the text.

near 852 eV and a broad multiplet near 854 eV, labeled as A and B respectively in Fig. 2. The bulk sensitive FY shows the same features indicating that the surface and bulk have the same electronic structure although they are less pronounced due to strong self-absorption at the L_3 edge[41]. Note that these spectra were aligned using a NiO standard which has a peak at 852 eV, which is close yet distinct from the multiplet labeled A. While not presented here, a change in valence from Ni^{3+} to Ni^{2+} due to oxygen non-stoichiometry (e. g. $\text{RNiO}_{3-\delta}$) occurs by an increase in the A peak intensity and gradual shifting to 852 eV while the B peak diminishes.

By treating the spectra as containing two main components, we have fit all the L_3 with a two Gaussian model to extract

the position of the two main multiplets. While the multiplets are clear in the insulating phase, there also exists features in the metallic state consistent with some remaining multiplet character, which is heavily screened by the metallic state. The results of this fit can be seen in Fig. 2(c) as a function of rare earth ion. A direct inspection of the Fig. shows the presence of two distinct well defined splittings depending on the metallic vs. insulating nature of the ground state of 1 eV (metallic) and 1.7 eV (insulating), respectively. The data of $\text{Nd}_{0.5}\text{Sm}_{0.5}$ is an outlier since at 300 K and are very close to the transition from the metallic to insulating phase. In previous work, we used a NiO_6 cluster calculation that connected the splitting of these features to the charge transfer energy, $\Delta^{(3)} = E(3d^8\bar{L}) - E(3d^7)$ [42]. This notion will be addressed in more detail in the Theory and Discussion sections below, and implies that there might be a discontinuous change in Δ across the MIT.

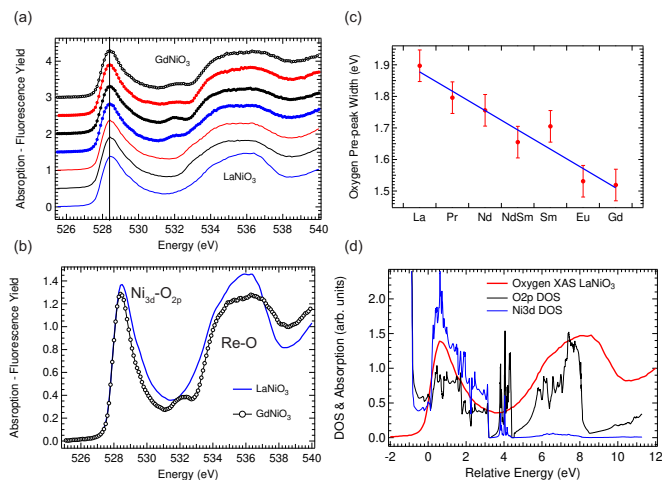


FIG. 3: (a) The oxygen K-edge spectra at 300K for the series from R = Gd to La with the $\text{Ni}_{3d}\text{-O}_{2p}$ marked by the vertical. (b) shows a comparison of the ends members of the measured series highlighting the pre-peak from hybridization with Ni and the second feature due Re-O hybridization. (c) This panel shows the FWHM of the pre-peak at 300K as a function of R. (d) Comparison between LaNiO_3 XAS and the oxygen projected density of states (DOS) from Ref. [43]

B. Oxygen K-edge Absorption

Due to the highly covalent nature of the bonding between Ni and O, probing the oxygen states is equally important to that of Ni. Figure 3 shows the oxygen K-edge absorption spectrum for the series shown in Fig. 1(a). In all cases the spectra are broadly defined by a sharp pre-peak around 529 eV due to Ni 3d and O 2p hybridization and a broad peak around 538 eV connected to mixing of the rare earth (R) states with oxygen. These spectra are in good agreement with other published data[37, 44–46] and are consistent with fully oxygenated case of RNiO_3 [45]. In this case we present only the bulk-sensitive FY since they suffer less from self-absorption and due the fact that the EY data for the insulating samples lead to difficulties in creating a consistent comparison be-

tween the data.

One of the main findings of this measurement is that the leading edge of the pre-peaks are all aligned and the changes occur only the higher energy side of the pre-peak. This is best seen in the comparison of the two ends of the series for Gd and La shown in Figure 3(b). Here we see that the main effect is the reduction in the pre-peak width and perhaps a drop in overall area size. Since small changes in the normalization of the oxygen spectra can influence the small changes in the pre-peak height, here we focus on the changes in the peak width across the series (Fig. 3(c)). As clearly seen, there is a linear trend that tracks well with the decreasing bandwidth across the RNiO_3 series inferred from changes in the bond angle[6, 11]. With the shrinking 3d bandwidth, the overlap with the 2p bands decreases as seen by the loss of pre-peak intensity at higher energy. An important aspect of the oxygen K-edge measurements is that due to the weak core-hole interaction at this edge, the XAS can be directly compared to the oxygen partial density of states[47–49]. To illustrate this point we consider the comparison of the LaNiO_3 XAS with the calculated density of states from Ref. [43]. As seen, there is the good agreement between the two that will be utilized during the discussion in connection to the underlying physics.

C. Case of NdNiO_3

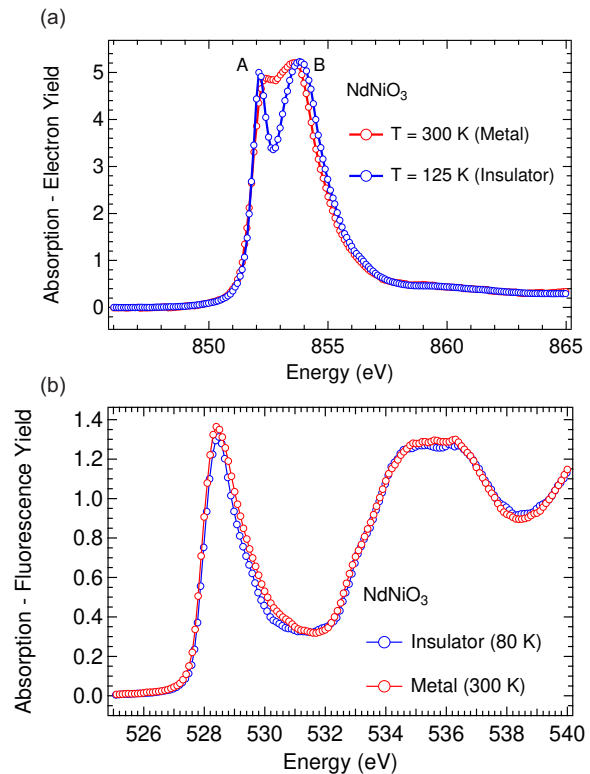


FIG. 4: (a) Ni L_3 edge below and above the MIT. (b) Corresponding oxygen K-edge in the metallic vs. insulating phases.

The situation of R = Nd offers a representative compound to

explore the spectroscopy of the insulating vs. metallic phases. As shown in Fig. 4, as a function of temperature the Ni L-edge across the MIT changes in the same manner as it does as a function of R. Specifically, below the MIT ($T_{MIT}=190$ K) there is an abrupt change in the XAS into the multiplet split phase of the Ni L-edge for NdNiO_3 , which is exactly the same as that of the other insulating phases. In this context, we can conjecture that understanding the spectra for the case of Nd should provide an understanding of all the other members in the series. For the case of oxygen, tracking the change in the same compound allows a quantitative comparison of the variation in the oxygen spectrum. As seen in Fig. 4, there is a narrowing of the pre-peak associated with the decrease of the Ni 3d bandwidth that results in a decrease of the overlap with the oxygen 2p states. The integrated area decreases by $\sim 15\%$ in the insulating phase. A similar analysis of the Ni L-edge is not as clear largely due to the change of the screening across the transition that complicates analysis of the total area of the spectrum.

At this point is worth noting that the same change occurs for the case of PrNiO_3 albeit at a lower temperature while for LaNiO_3 no noticeable change found in the L-edge spectrum at low temperature, which is consistent with the persistent metallic phase. For the case of R from Sm to Gd, we also looked for changes when crossing the low temperature transition into the E'-type AFM phase; no clear changes has been observed at the L-edge. This indicates that the fundamental change in the L-edge spectrum is connected with the transition into the insulating phase rather than to magnetism. In addition, the oxygen K-edge shows a very slight decrease in the pre-peak that will be discussed in more detail below.

D. Theory of the Ni L-edge X-ray Absorption Lineshape

The ground state of trivalent nickel compounds has been a long-standing discussion [37, 40, 50–53]. The question is directly related to the lowest electron-removal state of divalent nickel compounds. Historically $\text{Ni}(2+)\text{O}$ has been extensively studied in context of charge transfer insulators. The ground state of NiO is a high-spin triplet state with two holes in the e_g orbitals. Within octahedral symmetry (O_h), the ground state is 3A_2 and can be written as $|d_{x^2-y^2}\uparrow d_{3z^2-r^2}\uparrow\rangle$. NiO is known as a charge-transfer insulator with a gap of 4.3 eV [54]. The size of the insulating gap is directly related to the charge-transfer energy $\Delta^{(n)}$ for n holes, defined as

$$\Delta^{(2)} = E(d^9\bar{L}) - E(d^8), \quad (1)$$

where \bar{L} stands for a hole on the oxygen ligands. In order to reproduce the gap, a charge-transfer energy of 5.5-6.5 eV is needed. Since the Coulomb repulsion is of the same size, NiO is in fact very close to the boundary between a charge-transfer insulator and a Mott-Hubbard insulator [31]. This observation has important consequences for trivalent nickel compounds. Instead of a high-spin state favored by the Hund's exchange terms in the dd Coulomb interaction [50], the strong covalency stabilizes the low-spin state (2E in O_h) [52]. The strong covalency is due to the lowering of the charge-transfer energy

when the valency is increased. The charge-transfer energy for the trivalent system can, in a first approximation, be related to that of the divalent system via

$$\Delta^{(3)} = E(d^8\bar{L}) - E(d^7) \cong \Delta^{(2)} - U. \quad (2)$$

This situation is similar to copper oxides, which, with a charge-transfer energy of 2-3 eV, are clearly in the charge-transfer regime. For cuprates, the lowest electron-removal state is a singlet [55, 56] with predominantly $d^9\bar{L}$ character. When hole is doped in to a cuprate, these lowest electron-removal states, known as a Zhang-Rice singlet, are responsible for the conductivity. For nickelates the configuration of the lowest electron-removal state has mainly $|d_{e_g}^2\uparrow\bar{L}_{e_g\downarrow}\rangle$ character. The assignment of low-spin was further supported by O 1s X-ray absorption [51] that clearly showed a strong increase in the ligand-hole character with hole doping of NiO via Li substitution. In addition, the $2p \rightarrow 3d$ X-ray absorption could only be interpreted following the assumption that the additional holes couple antiparallel to the spin on the nickel ion [57].

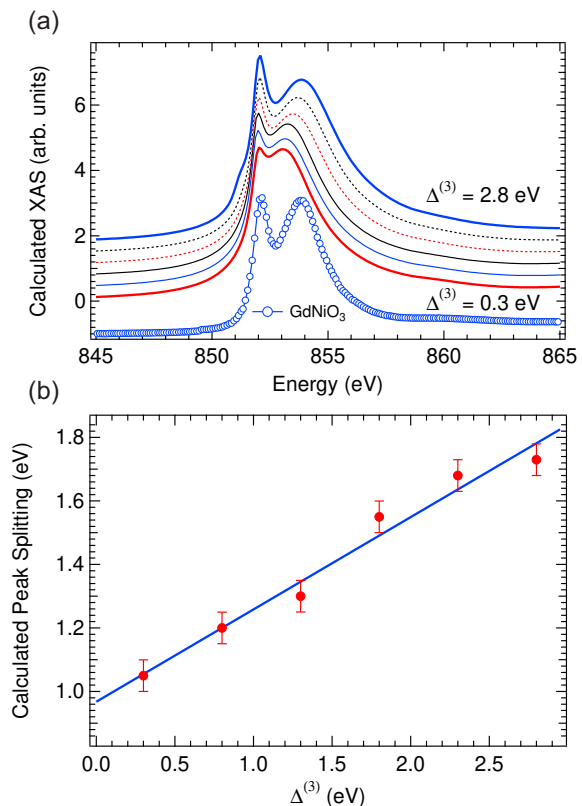


FIG. 5: (a) Calculated absorption spectra for Ni^{3+} in a NiO_6 cluster as a function of the charge transfer energy, $\Delta^{(3)}$. Included is a comparison with the Ni L-edge of GdNiO_3 in the insulating phase. (b) The A-B peak splitting described in Fig. 2 extracted from the calculated spectra as a function of $\Delta^{(3)}$. The line is a linear fit to the results.

Following this idea, calculations were performed for a NiO_6 cluster with octahedral coordination using the methods

described in Ref. [53]. The Hamiltonian includes the on-site Coulomb between the $3d$ electrons and between the $3d$ electrons and the $2p$ core hole. The parameters are calculated within the Hartree-Fock limit and scaled down to 80% to account for intra-atomic screening effects. The monopole parts were $F_{dd}^0 = 6$ eV and $F_{pd}^0 = 7$ eV. The spin-orbit coupling was included for the $3d$ and $2p$ electrons. The hybridization with the ligands was taken into account by including configurations up to double ligand hole. The hybridization parameter is $V = 2.25, -1.03$ eV for the e_g and t_{2g} orbitals, respectively. The cubic crystal field $10Dq$ is 1.5 eV.

Despite its relative simple appearance, the L -edge spectra for trivalent nickel compounds are significantly more difficult to interpret than those for divalent nickel systems, such as NiO. As seen in Fig ???, the spectra consist of a sharp peak at the low-energy side of the edge, followed at higher energy by a broad feature. These broadenings are difficult to explain by multiplet effects with a constant broadening and indicate the presence of additional broadening effects. First, it is important to note that the sharp features often found at the L -edges in transition-metal compounds are due to the creation of an excitonic state below the continuum states by the strong Coulomb attraction between the $2p$ core hole and the $3d$ electrons. The energy needed to transfer an electron from the ligands to the transition-metal in the XAS final states is given $\Delta^{(n)} - U_c + U$. Since generally $U_c > U$, the effective charge-transfer is lower in the XAS final states compared to the ground state. For divalent nickel oxides, such as NiO, $\Delta^{(2)} \cong 5.5 - 6.5$ eV, and this difference is not too important. However, for trivalent nickel oxides the charge-transfer energy is approximately $\Delta^{(3)} \cong 0 - 3$ eV. This means that, in particular, the high-energy final states can overlap with the continuum states. The dramatic effects of coupling to the continuum were apparent in non-resonant inelastic x-ray scattering on rare-earth compounds [58], where the substantial broadening in addition to the usual core-hole lifetime broadening was observed for states at higher energies. This coupling to the continuum can be included by having the Lorentzian broadening increase parabolically from the core-hole broadening due to Auger effects of 0.25 eV at the absorption edge to 1.25 eV at 1 eV above the edge. Assuming that the coupling to the continuum does not vary strongly this broadening is then kept constant.

Figure 5 shows the change in spectral line shape as a function of charge-transfer energy. Decreasing the charge-transfer energy makes the system more covalent. In the final state, the $1s3d^9L$ states will be closer in energy to the $1s3d^8$ configurations. The closer proximity increases the hybridization between these states leading to a compression of the spectral features[59]. At the L_3 edge, the decrease in covalency increases the energy separation between the two features. At the L_2 edge, an increase in charge-transfer energy leads to the development of a more pronounced shoulder at the low-energy side. These trends correspond well to the trends observed experimentally in Ref. [40] and in Fig. 5. In metallic systems with $RE = \text{Nd}$ or Pr at low temperatures, the covalency is stronger and no clear separation of the features in the L_3 edge is observed. For insulators with $R = \text{Eu}, \text{Y}, \text{Lu}$, on the other hand, the L_3 is clearly split into two features.

IV. DISCUSSION

In this section, we begin with a quick summary of the key features observed in our measurements. As shown above, one of the key questions concerns understanding the role of the $3d^8L$ character in the ground state of nickelates and the data analysis requires to include this state to reproduce the observed XAS features. As noted by Mizokawa et al.[16], nickelates should really be viewed as a self-doped Mott insulator, where the doping comes from the oxygen $2p$ band[60]. Certainly understanding the spectroscopy necessitates the inclusion of a significant $3d^8L$ component to reproduce a similar spectrum from the calculations. As seen above in the Ni L -edge data, the key factor in the change of the spectrum shown in Figs. 2 and 4 is the transition from the metallic to insulating phase. In the calculations shown in Figure 5, the splitting between the A and B multiplets is directly influenced by the charge transfer energy, $\Delta^{(3)}$. An interesting suggestion is that the change between the features in the metallic vs. insulating phases could be due to a change in $\Delta^{(3)}$. Since the charge transfer energy is closely tied to the splitting of the $3d$ and $2p$ levels, perhaps as a gap opens there is an increase in the offset of these states. However, the small nature of the gap[32–36] might suggest that screening in the metallic phase also plays a role since there is a Madelung term in the derivation of the charge transfer energy[61] that could be affected by free-carriers and covalency.

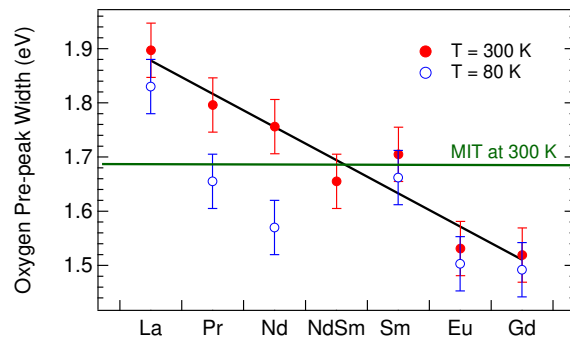


FIG. 6: The $\text{Ni}_{3d}\text{-O}_{2p}$ oxygen pre-peak width as a function of R and temperature. The green line marks the extrapolated width for the case of an MIT at 300K.

From the oxygen site perspective, the strong pre-peak also indicates a significant $3d^8L$ contribution to the ground-state wave function. Unlike the Ni L -edge data that undergoes a profound change in lineshape, the K-edge is much more subtle and in line with the energy scale of the physics that splits the metallic vs. insulating phases. Within 50 meV, there is no observable increase in the energy of the leading edge that has been observed in other systems where gaps open[62–65]. For the case of oxygen all of the changes occur on the high energy side and result in a decreased peak-width (and correspondingly peak area) consisted with the reduction in $d - p$ overlap resulting from a bandwidth reduction. Since the peak

area is proportional to the $3d^8\bar{L}$ component, this indicates the reduction in the ligand hole content both as a function of R and across the MIT. This is clearly seen in Fig. 6, where we have included the low temperature data for the pre-peak width. For the cases where the system always stays metallic, there is also a slight decrease in the width, although it is just outside the error bars and might not be real. For the R = Sm, Eu, Gd, there is no change when crossing the magnetic transition indicating the primary effect in the bandwidth reduction occurs at the MIT. For the cases of Pr and Nd, there is a clear drop in the pre-peak width associated with a reduction of $3d^8\bar{L}$ spectral weight.

While band effects play a very important role here, by starting from the ionic perspective the wave function can be written as:

$$|Ni^{3+}\rangle = \alpha|3d^7\rangle + \beta|3d^8\bar{L}\rangle + \gamma|3d^9\bar{L}^2\rangle + \dots \quad (3)$$

which implies that a reduction in the ligand hole terms will lead to an increase in the $3d^7$ component. This is basically the idea first promoted by Sarma et al. [30], that changes in the $p-d$ hybridization can move the metal to insulator line in the ZSA diagram. More recent work with DFT-DMFT[66], presented a similar diagram from the perspective of the local count of the $3d$ electrons, N_d . In this self-doped case, a reduction in the ligand hole components could reduce N_d and push the system across the MIT boundary if it were at the close proximity. From the perspective of this picture, one might imagine that there is a critical value of the ligand hole weight below which the system becomes insulating as highlighted by the green line in Fig. 6. This also connects with the recent results that suggest there could be a *pre-formed* bond-disproportionated state even in the metallic phase[67–69]. In the future, we hope to develop better ways to model these spectra in order to quantitatively assess these changes to better

understand the physics of the MIT in the rare-earth nickelates and other complex oxides in the charge-transfer regime.

V. CONCLUSION

In conclusion, we have highlighted the importance of the $3d^8\bar{L}$ state in order to understand the details of the Ni L- and O K- edge spectra of the perovskite nickelates. Given the detailed knowledge that exists about the physical properties as a function of rare earth ion, R, we hope that the systematics of this data can aid in building a better picture of the physics of co-existing charge and magnetic orders that result in a metal to insulator transition.

VI. ACKNOWLEDGEMENTS

This article is dedicated to D.D. Sarma whose discussions, insight and invaluable comments concerning this data over the last several years have made this paper possible. The authors thank Bogdan Dabrowski for providing the high-quality RNiO₃ samples. Work at the Advanced Photon Source, Argonne National Laboratory was supported by the U.S. Department of Energy, Office of Science under Grant No. DEAC02-06CH11357. MvV was supported by the U. S. Department of Energy (DOE), Office of Basic Energy Sciences, Division of Materials Sciences and Engineering under Award No. DE-FG02-03ER46097 and NIU's Institute for Nanoscience, Engineering, and Technology. The work at the University of Arkansas is funded in part by the Gordon and Betty Moore Foundations EPiQS Initiative through Grant GBMF4534 and by the DOD-ARO under Grant No. 0402-17291.

-
- [1] J. Goodenough, Reports On Progress In Physics **67**, 1915 (2004).
- [2] E. Dagotto, Science **309**, 257 (2005).
- [3] M. Imada, A. Fujimori, and Y. Tokura, Reviews Of Modern Physics **70**, 1039 (1998).
- [4] M. Medarde, JOURNAL OF PHYSICS CONDENSED MATTER (1997).
- [5] G. Catalan, Phase Transitions **81**, 729 (2008).
- [6] J. Zhou and J. Goodenough, Physical Review B **69**, 153105 (2004).
- [7] A. Wold, B. Post, and E. Banks, Journal Of The American Chemical Society **79**, 4911 (1957).
- [8] J. B. Goodenough and P. M. Raccah, Journal Of Applied Physics **36**, 1031 (1965).
- [9] G. Demazeau, A. Marbeuf, M. Pouchard, and P. Hagenmuller, Journal of Solid State Chemistry **3**, 582 (1971).
- [10] J. K. Vassiliou, M. Hornbostel, R. Ziebarth, and F. J. Disalvo, Journal of Solid State Chemistry **81**, 208 (1989).
- [11] J. Torrance, P. Lacorre, A. Nazzal, E. Ansaldo, and C. Niedermayer, Physical Review B **45**, 8209 (1992).
- [12] J. Rodríguez-Carvajal, S. Rosenkranz, M. Medarde, P. Lacorre, M. Fernandez-Díaz, F. Fauth, and V. Trounov, Physical Review B **57**, 456 (1998).
- [13] M. Medarde, P. Lacorre, K. Conder, F. Fauth, and A. Furrer, Physical Review Letters **80**, 2397 (1998).
- [14] U. Staub, G. Meijer, F. Fauth, R. Allenspach, J. Bednorz, J. Karpinski, S. Kazakov, L. Paolasini, and F. d'Acapito, Physical Review Letters **88**, 126402 (2002).
- [15] V. Scagnoli, U. Staub, M. Janousch, A. Mulders, M. Shi, G. Meijer, S. Rosenkranz, S. Wilkins, L. Paolasini, J. Karpinski, et al., Physical Review B **72**, 155111 (2005).
- [16] T. Mizokawa, D. I. Khomskii, G. Sawatzky, and S. Johnston, Physical review B. Condensed matter and materials physics **61**, 11263 (2000).
- [17] I. I. Mazin, D. I. Khomskii, R. Lengsdorf, J. Alonso, W. G. Marshall, R. A. Ibberson, A. Podlesnyak, M. J. Martinez-Lope, M. M. Abd-Elmeguid, and S. Johnston, Physical Review Letters **98**, 176406 (2007).
- [18] H. Park, A. Millis, C. A. Marianetti, and S. Johnston, Physical Review Letters **109**, 156402 (2012).
- [19] S. Johnston, A. Mukherjee, I. Elfimov, M. Bericu, and G. A. Sawatzky, Physical Review Letters **112**, 106404 (2014).
- [20] J. L. García-Muñoz, J. Rodríguez-Carvajal, and P. Lacorre, EPL (Europhysics Letters) **20**, 241 (1992).

- [21] V. Scagnoli, U. Staub, A. Mulders, M. Janousch, G. Meijer, G. Hammerl, J. Tonnerre, and N. Stojic, *Physical Review B* **73**, 100409 (2006).
- [22] V. Scagnoli, U. Staub, Y. Bodenthin, M. Garcia-Fernandez, A. M. Mulders, G. I. Meijer, and G. Hammerl, *Physical Review B* **77**, 115138 (2008).
- [23] U. Staub, M. García-Fernández, A. M. Mulders, Y. Bodenthin, M. J. Martínez-Lope, and J. A. Alonso, *JOURNAL OF PHYSICS CONDENSED MATTER* **19**, 092201 (2007).
- [24] Y. Bodenthin, U. Staub, C. Piamonteze, M. Garcia-Fernandez, M. J. Martinez-Lope, and J. A. Alonso, *JOURNAL OF PHYSICS CONDENSED MATTER* **23**, 036002 (2011).
- [25] J. Zhou, J. Goodenough, and B. Dabrowski, *Physical Review B* **67**, 020404 (2003).
- [26] D. Kumar, K. P. Rajeev, J. A. Alonso, and M. J. Martínez-Lope, *Physical Review B* **88**, 014410 (2013).
- [27] J. S. Zhou and J. Goodenough, *Physical review B. Condensed matter and materials physics* **89**, 245138 (2014).
- [28] D. D. Sarma, N. Shanthi, and P. Mahadevan, *JOURNAL OF PHYSICS CONDENSED MATTER* **6**, 10467 (1994).
- [29] J. Zhou, J. Goodenough, and B. Dabrowski, *Physical Review B* **70**, 081102 (2004).
- [30] S. Barman, A. Chainani, and D. Sarma, *Physical Review B* **49**, 8475 (1994).
- [31] J. Zaanen, G. Sawatzky, and J. Allen, *Physical Review Letters* **55**, 418 (1985).
- [32] M. Medarde, D. Purdie, M. Grioni, M. Hengsberger, Y. Baer, and P. Lacorre, *EPL (Europhysics Letters)* **37**, 483 (1997).
- [33] I. Vobornik, L. Perfetti, M. Zacchigna, M. Grioni, G. Margaritondo, J. Mesot, M. Medarde, and P. Lacorre, *Physical Review B* **60**, R8426 (1999).
- [34] K. Okazaki, T. Mizokawa, and A. Fujimori, *Physical Review B* **67**, 73101 (2003).
- [35] E. F. Schwier, R. Scherwitzl, Z. Vydrova, M. Garcia-Fernandez, M. Gibert, P. Zubko, M. G. Garnier, J. M. Triscone, and P. Aebi, *Physical Review B* **86**, 195147 (2012).
- [36] T. Katsufuji, Y. Okimoto, T. Arima, Y. Tokura, and J. B. Torrance, *Physical Review B* **51**, 4830 (1995).
- [37] T. Mizokawa, A. Fujimori, T. Arima, Y. Tokura, and N. Mori, *Physical Review-Section B-Condensed Matter* **52**, 13865 (1995).
- [38] S. Lee, R. Chen, and L. Balents, *Physical Review Letters* **106**, 016405 (2011).
- [39] A. Subedi, O. E. Peil, and A. Georges, *Physical Review B* **91**, 75128 (2015).
- [40] C. Piamonteze, F. de Groot, and H. Tolentino, *Physical Review B* **71**, 020406 (2005).
- [41] G. van der Laan and A. I. Figueroa, *Coordination Chemistry Reviews* **277-278**, 95 (2014).
- [42] J. Liu, S. Okamoto, M. Van Veenendaal, M. Kareev, B. Gray, P. Ryan, J. Freeland, and J. Chakhalian, *Physical Review B* **83**, 161102 (2011).
- [43] G. Gou, I. Grinberg, A. M. Rappe, and J. M. Rondinelli, *Physical Review B* **84**, 144101 (2011).
- [44] M. Medarde, A. Fontaine, J. García-Muñoz, J. Rodríguez-Carvajal, M. De Santis, M. Sacchi, G. Rossi, and P. Lacorre, *Physical Review B* **46**, 14975 (1992).
- [45] M. Abbate, G. Zampieri, F. Prado, and A. Caneiro, *Physical Review B* **65**, 155101 (2002).
- [46] J. Suntivich, W. T. Hong, Y.-L. Lee, J. M. Rondinelli, W. Yang, J. B. Goodenough, B. Dabrowski, J. W. Freeland, and Y. Shao-Horn, *Journal Of Physical Chemistry C* **118**, 1856 (2014).
- [47] D. Sarma, N. Shanthi, and P. Mahadevan, *Physical Review B* **54**, 1622 (1996).
- [48] F. de Groot, *Coordination Chemistry Reviews* **249**, 31 (2005).
- [49] S. Medling, Y. Lee, H. Zheng, J. F. Mitchell, J. W. Freeland, B. N. Harmon, and F. Bridges, *Physical Review Letters* **109**, 157204 (2012).
- [50] A. Fujimori and F. Minami, *Physical Review B* **30**, 957 (1984).
- [51] P. Kuiper, G. Kruizinga, J. Ghijsen, G. Sawatzky, and H. Verweij, *Physical Review Letters* **62**, 221 (1989).
- [52] J. Van Elp, H. Eskes, P. Kuiper, and G. Sawatzky, *Physical Review B* **45**, 1612 (1992).
- [53] M. Van Veenendaal and G. Sawatzky, *Physical Review Letters* **70**, 2459 (1993).
- [54] G. Sawatzky and J. Allen, *Physical Review Letters* **53**, 2339 (1984).
- [55] F. Zhang and T. Rice, *Physical Review B* **37**, 3759 (1988).
- [56] H. Eskes and G. Sawatzky, *Physical Review Letters* **61**, 1415 (1988).
- [57] M. Van Veenendaal and G. Sawatzky, *Physical Review B* **50**, 11326 (1994).
- [58] R. A. Gordon, G. T. Seidler, T. T. Fister, M. W. Haverkort, G. A. Sawatzky, A. Tanaka, and T. K. Sham, *EPL (Europhysics Letters)* **81**, 26004 (2008).
- [59] G. Van Der Laan, J. Zaanen, G. Sawatzky, R. Karnatak, and J.-M. Esteve, *Physical Review B* **33**, 4253 (1986).
- [60] A. V. Ushakov, S. V. Streltsov, and D. I. Khomskii, *JOURNAL OF PHYSICS CONDENSED MATTER* **23**, 445601 (2011).
- [61] Y. Ohta, T. Tohyama, and S. Maekawa, *Physical Review B* **43**, 2968 (1991).
- [62] A. Cavalleri, H. H. W. Chong, S. Fourmaux, T. E. Glover, P. A. Heimann, J. C. Kieffer, B. S. Mun, H. A. Padmore, and R. W. Schoenlein, *Physical Review B* **69**, 153106 (2004).
- [63] A. Cavalleri, M. Rini, H. H. W. Chong, S. Fourmaux, T. E. Glover, P. A. Heimann, J. C. Kieffer, and R. W. Schoenlein, *Physical Review Letters* **95**, 067405 (2005).
- [64] M. Merz, G. Roth, P. Reutler, B. Büchner, D. Arena, J. Dvorak, Y. U. Idzerda, S. Tokumitsu, and S. Schuppler, *Physical Review B* **74**, 184414 (2006).
- [65] M. Rini, Y. Zhu, S. Wall, R. I. Tobey, H. Ehrke, T. Garl, J. W. Freeland, Y. Tomioka, Y. Tokura, A. Cavalleri, et al., *Physical Review B* **80**, 155113 (2009).
- [66] X. Wang, M. Han, L. de Medici, H. Park, C. Marianetti, and A. Millis, *Physical Review B* **86**, 195136 (2012).
- [67] C. Piamonteze, H. Tolentino, A. Ramos, N. Massa, J. Alonso, M. Martinez-Lope, and M. Casais, *Physical Review B* **71**, 012104 (2005).
- [68] M. Medarde, C. Dallera, M. Grioni, B. Delley, F. Vernay, J. Mesot, M. Sikora, J. A. Alonso, and M. J. Martínez-Lope, *Physical Review B* **80**, 245105 (2009).
- [69] R. Jaramillo, S. D. Ha, D. M. Silevitch, and S. Ramanathan, *Nature Physics* **10**, 304 (2014).